Alqalam Journal of Medical and Applied Sciences. 2025;8(4):2851-2857
https://doi.org/10.54361/ajmas.2584110

Original article

Formulation of a Floating Drug Delivery System for Sustained Release Delivery of Methotrexate Using *Manihot Esculenta* Starch

Yinka J Oyeniyi[1*], Emmanuel C Omenazu[1], Rabiu TG[2], Andrew Onu[3]

[1]*Department of Pharmaceutics and Pharmaceutical Technology, Faculty of Pharmaceutical Sciences, Usmanu Danfodiyo University, Sokoto, Sokoto State, Nigeria.*
[2]*Department of Pharmacology and Toxicology, Faculty of Pharmaceutical Sciences, Usmanu Danfodiyo University, Sokoto, Sokoto State, Nigeria.*
[3]*Department of Medical Biochemistry, Faculty of Basic Medical Sciences, Usmanu Danfodiyo University, Sokoto, Sokoto State, Nigeria.*
Corresponding author. professordeyinkajoyeniyi@gmail.com

Abstract
The management of rheumatoid arthritis (RA) using methotrexate (MTX) is limited by poor oral bioavailability, dose-dependent toxicity, and gastrointestinal side effects. This study aimed to formulate and evaluate a methotrexate floating drug delivery system (FDDS) using *Manihot esculenta* (cassava) starch as a natural polymer to enhance gastric retention and sustain drug release. Cassava starch was extracted and characterized before its use in the preparation of floating microspheres via the ionic gelation method. Microspheres were formulated using pregelatinized cassava starch and sodium alginate with varying polymer ratios (1:1 and 1:2) and stirring speeds (300 and 600 rpm). The microspheres were evaluated for physicochemical and micromeritic properties, buoyancy, swelling index, floating lag time, total floating duration, entrapment efficiency, and in vitro drug release kinetics. All formulations exhibited good flow and spherical morphology. Floating lag times ranged from 2.8 to 4.4 min, with total floating durations exceeding 19 h. Entrapment efficiencies ranged from 57% to 81%, and swelling indices from 152% to 259%. In-vitro drug release profiles indicated sustained release over 18 h, best fitting the zero-order (R^2 = 0.992–0.997) and Korsmeyer-Peppas (R^2 = 0.986–0.993) models, suggesting super case-II transport dominated by polymer relaxation and erosion. Optimized cassava starch-based floating microspheres demonstrated prolonged gastric retention and sustained MTX release, highlighting the potential of *Manihot esculenta* starch as a biodegradable, cost-effective polymer for enhancing oral methotrexate therapy in RA management.
Keywords. Methotrexate, Floating Drug Delivery, Cassava Starch, Rheumatoid Arthritis.

Introduction

Oral drug delivery is the most preferred route of administration due to its convenience, patient compliance, and cost-effectiveness [1]. However, conventional oral dosage forms are often limited by short gastric residence time and variable drug absorption, particularly for drugs with narrow absorption windows or poor solubility [2]. Floating drug delivery systems (FDDS) have emerged as an effective gastroprotective approach designed to prolong gastric retention, enhance drug bioavailability, and achieve sustained release profiles [3].

Methotrexate, a folate antagonist widely used in the management of Rheumatoid Arthritis (RA), Multiple Sclerosis, Vasculitis, Systemic Lupus Erythematosus, Psoriasis, Inflammatory Bowel Disease, and Juvenile Idiopathic Arthritis [4]. The various clinical applications of methotrexate are limited by some intrinsic features of the molecule, thereby impeding its clinical potential [5]. The aqueous solubility of methotrexate is low (<0.001 mg/mL) and has a low permeability across biological membranes, resulting in decreased systemic bioavailability with increasing doses.

In clinical practice, adverse effects are a common reason for dose reduction or discontinuation of methotrexate therapy. Many studies report that intolerance or toxicity is among the leading causes of methotrexate withdrawal in long-term treatment [6]. Formulating an FDDS could help mitigate these challenges of low solubility, erratic absorption, dosing frequency, therapeutic inefficacy, and dose-dependent side effects [7].

Natural polymers are increasingly gaining attention as drug excipients because they are safe, biodegradable, and cost-effective excipients in drug delivery [8]. Cassava (*Manihot esculenta*) is a shrubby plant belonging to the family Euphorbiaceae. Cassava is extensively cultivated as an annual crop in tropical and subtropical regions for its edible starchy tuberous root, a major source of carbohydrates [9]. Starch isolated from *Manihot esculenta* (cassava) is abundant, biocompatible, and has been reported to exhibit favorable physicochemical properties, making it suitable for sustained-release formulations [10]. Its application in floating systems not only offers a novel use of indigenous biopolymers but also aligns with the global drive for eco-friendly and sustainable pharmaceutical excipients.

This study, therefore, focuses on the formulation and evaluation of a floating drug delivery system for sustained release delivery of methotrexate using *Manihot esculenta* starch as a natural polymeric matrix.

Received*: 10-10-2025 -* ***Accepted****: 08-12-2025 -* ***Published****: 16-12-2025*

Materials and Methods

Materials

Methotrexate BP (API Rochem International Inc USA), Sodium bicarbonate (Sisco Research Laboratories Pvt Ltd, Mumbai India), Calcium carbonate (Chemie Pvt, Ltd, Mumbai India), Sodium alginate (BDH Ltd, Poole England), Sodium metabisulfite (BDH Chemicals Ltd, Poole, England), and Sodium Hydroxide (Finar Chemicals Ltd., Ahmedabad, India).

Methods

Collection and Identification of Plants

Tubers of Manihot esculenta were collected from the Kara Area, Sokoto, Sokoto State, and identified at the Herbarium, Usmanu Danfodiyo University, Sokoto. Herbarium with Number UDUH/ANS/0615.

Extraction of Cassava Starch

The procedure described in the literature was adopted with little modification. The cassava tuber was peeled and cut into cubes, and 20 Kg was weighed. The cassava tubers were then separately soaked in 10 liters 0.0075 % of sodium metabisulfite solution overnight to avoid oxidation. The mixture was then milled, stirred, and filtered using double-fold clean cheesecloth. This was allowed to settle while the starch sediments completely. This was followed by decanting the water and centrifuging the suspension at 4000 rpm for 5 min using a Lab centrifuge. After centrifugation, the starch was separated from water and non-water constituents. Finally, the pure starch obtained from centrifugation was air-dried in a hot oven (Nurve FN055 oven, Germany), size-reduced with a grinder (Super Master Co. Ltd. SMB-3377), and sifted through Sethi standard sieves. The flour cassava starch was then packed into an airtight container and stored at room temperature for further analysis and characterization [11].

Formulation Studies

Pregelatinized cassava starch was prepared using the method of Odeku *et al.* (2019). Aqueous starch slurry (20 % w/v) was heated over a water bath with continuous stirring for 15 min until a clear paste was formed. Formulation studies were carried out to determine the ability of pregelatinized cassava starch in combination with sodium alginate to form stable spherical microspheres. Several formulations were prepared using varying ratios of freshly pregelatinized cassava starch in combination with sodium alginate, chelating agents (calcium chloride) at 2% w/v concentration, stirring speed (300/600 rpm), and curing time (30 min) until stable microspheres were formed with gel blends of pregelatinized cassava [12,13].

Table 1. Formulation Design

Formulations	Ratio of Sodium alginate to Sodium bicarbonate	Speed of Rotation
F3	1:2	300
F2	1:1	600
F4	1:2	600
F1	1:1	300

Preparation of Methotrexate Microspheres

Cassava starch, 50 g, and 25 g of methotrexate were weighed and poured into a clean, dry beaker. Freshly prepared polymer blend of sodium alginate and (2% w/w) of sodium bicarbonate was prepared in a ratio of 1:1 and 1:2, respectively. The admixture was thoroughly mixed with a sufficient quantity of water to make a paste. The resulting dispersion was extruded into a beaker containing calcium chloride solution (2% w/v) using a 21G syringe needle at a stirring speed of 300/600 rpm. The formed microspheres were allowed to stand for 30 min for curing and then left to stand for 1 hour to allow further crosslinking of the polymers. The microspheres were collected by decantation, washed with distilled water, and then dried for 24 h in a hot air oven at 40 °C [14,15].

Characterization of Microspheres

Flow Characterization

The flow properties of prepared microspheres were investigated by measuring the bulk density, tapped density, and Carr's index. The bulk and tapped densities were measured in a 100 ml graduated measuring cylinder. The sample contained in the measuring cylinder was tapped. The initial bulk volume and final tapped volume were noted, from which their respective densities were calculated [16].

Bulk density & Tapped density

A 20.0 g quantity of each of the powder samples was placed in a 100 ml clean, dry measuring cylinder, and the volume, V_o, occupied by each of the samples without tapping was determined. After 200 taps occupied volumes, V_{200}, were determined. The bulk and tap densities were calculated as the ratio of weight to volume (V_o and V_{200}, respectively). The density (Bulk and tapped) was then determined using the expression below.

Received*: 10-10-2025 -* ***Accepted****: 08-12-2025 -* ***Published****: 16-12-2025*

$P_B = \frac{M}{Vo}$..... (1)

$P_T = \frac{M}{V200}$..... (2)

Where P_T is the tapped density, and P_B is the bulk density [17].

Compressibility Index CI

The CI of the powder was determined from the bulk and tap density as follows:

Percentage Compressibility = $\frac{(\text{Tapped density} - \text{bulk density})}{\text{Tapped density}}$ x 100..... (3)

[18,19].

Hausner's ratio

This was calculated as the ratio of tap density to bulk density of the samples using the equation below

Hausner's ratio = $\frac{\text{Tapped density}}{\text{Bulk Density}}$ ..... (4)

[20,21].

Angle of repose

The static angle of repose was determined using the Vanier scale method, where a stopper and a cylindrical aluminum tube were coupled together, and 5 g of the powder was poured into the cylinder, after which the cylinder was removed to allow the powder to flow on the stopper, forming a cone at the top. The hypotenuse was measured using the Vanier scale, and the angle of repose was calculated using the equation:

Tan θ = $\frac{opp}{adj}$..... (5)

Adj = $\frac{d}{2}$..... (6)

In Equation 5, opp is the distance exhibited by the powder from the base of the stopper to the tip of the powder heap, and Adj is the diameter of the stopper.

In Equation 6: Adj is the diameter formed by the powder divided by two (2).

[22].

Size and morphology

The particle size of the microspheres was determined using a Vanier caliper. The surface morphology of the microsphere was analyzed by scanning electron microscopy. The microspheres were sputtered with gold, and their morphology and surface characteristics were analyzed using scanning electron microscopy at an accelerating voltage of 25 KV [23,24].

Buoyancy studies

The floating capability of the microspheres was determined by placing the microspheres in a dissolution apparatus containing 900 mL of 0.1 N HCl, pH 1.2. The floating lag time (FLT) is the time for the microspheres to rise to the surface and float, while the total floating time (TFT) is the duration the microspheres remained on the surface of the medium [23].

Swelling index

Microspheres (100 mg) were soaked in 20 mL of phosphate buffer, pH 6.8, and the final weight after 3hours was determined. The swelling index was calculated using equation 7, [25,26].

Swelling Index (%) = $\frac{\text{Change in weight (mg)}}{\text{original weight (mg)}}$ x 100..... (7)

Determination of Entrapment Efficiency

The entrapment efficiency was determined by accurately weighing 50 mg of microspheres into a glass mortar and crushing them with a pestle. The crushed microspheres were suspended in 10 mL of phosphate buffer, pH 6.8. After 24hrs., the solution was filtered, and the filtrate was appropriately diluted using phosphate buffer, pH 6.8, and analyzed spectrophotometrically at 303 nm using a UV spectrophotometer [24].

The drug entrapment efficiency (E) was calculated using the formula

E = $\frac{\text{Practical drug content (mg)}}{\text{Theoretical drug content (mg)}}$ x 100..... (8)

Determination of drug release mechanism

The *in-vitro* dissolution studies were carried out using the paddle method, rotated at 50 rpm in 900 mL of phosphate buffer, pH 6.8, maintained at 37 ± 0.5°C. The microspheres (100 mg) were placed in the dissolution medium, and samples (5 ml) were withdrawn at different intervals and replaced with equal amounts of fresh medium. The sample was diluted, and the amount of methotrexate released was determined at a wavelength of 303 nm, using a UV/Visible spectrophotometer [24,27].

Received: *10-10-2025* - ***Accepted***: *08-12-2025* - ***Published***: *16-12-2025*

Table 2. Physicochemical properties of extracted starch from Manihot esculenta

Parameters	Cassava Starch
Yield Value (%)	43.10
Taste	Slight characteristic taste
Odour	No characteristic odour
Colour	White
Identification	Turns violet-blue with iodinated zinc chloride
Solubility	insoluble in cold water, soluble in hot water

Table 3. Flow characterization of the optimized microsphere

S/N	Formulations	Angle of repose θ	Bulk density g/cm³	Tapped density g/cm³	Hausner ratio	Carr's Index %
1	F1	26.93±0.11	0.57±0.01	0.71±0.04	1.24±0.01	19.72
2	F2	24.90±0.41	0.55±0.02	0.67±0.03	1.22±0.02	17.91
3	F3	25.83±0.28	0.55±0.01	0.70±0.01	1.27±0.03	21.43
4	F4	25.46±0.32	0.54±0.03	0.73±0.03	1.35±0.01	26.03

Table 4. Determination of the particle size, swelling index, floating lag time, floating time, and the entrapment efficiency of the optimized microsphere

S/N	Formulation	Particle size	Swelling index	Floating lag time	Floating time	Entrapment Efficiency
1	F1	3.01±0.26	259±16.09	2.80±0.30	23.30±0.26	57.00±0.5
2	F2	3.85±0.35	166±12.88	4.31±0.07	20.70±0.26	79.20±0.6
3	F3	3.25±0.24	227±15.06	3.28±0.13	22.40±0.40	68.20±0.2
4	F4	3.89±0.59	152±12.31	4.37±0.08	19.90±0.15	81.40±0.1

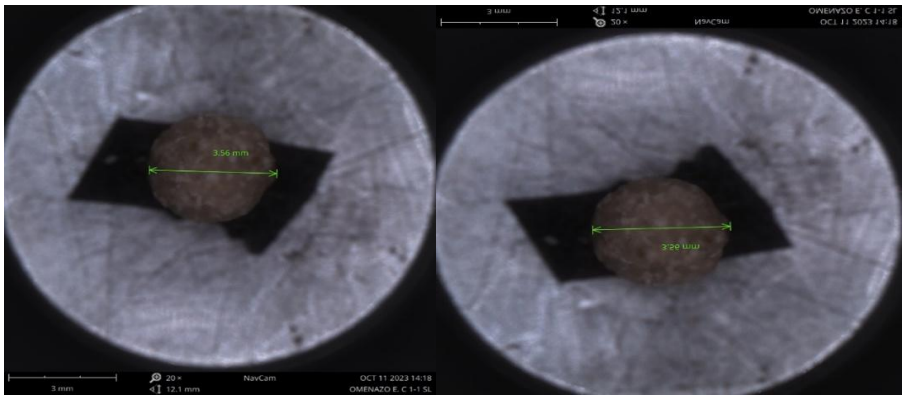

Fig 1. SEM image showing the shape and the surface characteristics of a floating microsphere containing cassava starch, sodium alginate, 1:1 sodium bicarbonate, speed rotation of 300 and 600

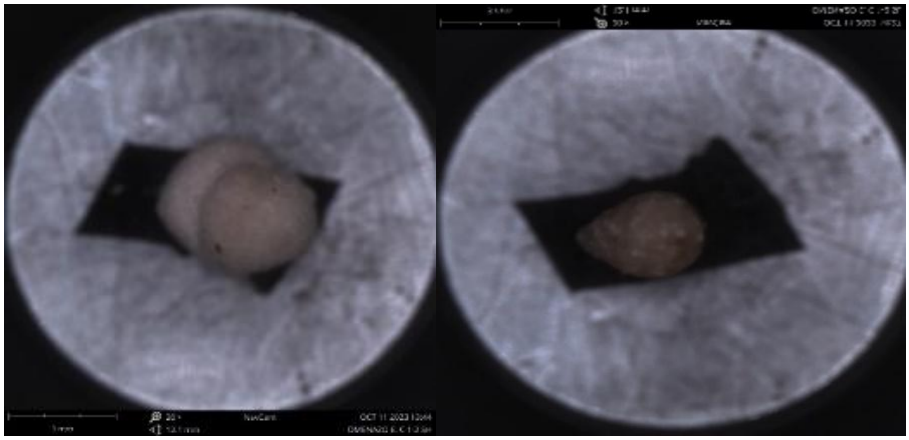

Fig 2. SEM image showing the shape and the surface characteristics of a floating microsphere containing cassava starch, sodium alginate, 1:2 sodium bicarbonate, speed rotation of 300 and 600

Received*: 10-10-2025 -* ***Accepted****: 08-12-2025 -* ***Published****: 16-12-2025*

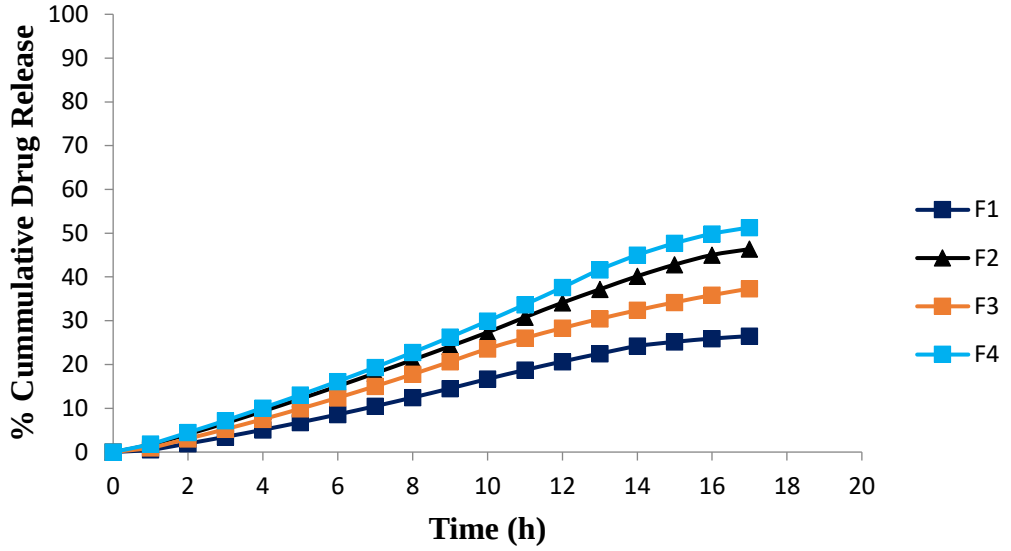

Figure 3. In-vitro Drug Release of microsphere

Table 5. Shows the kinetic model of the release of drugs from the microsphere

Formulations	Model							
	Zero Order		First Order		Korsmeyer Peppas		Higuchi	
	K_0	R^2	K_1	R^2	N	R^2	K_H	R^2
F1	1.767	0.992	0.103	0.559	1.300	0.987	7.857	0.910
F2	2.915	0.997	0.103	0.545	1.254	0.988	13.130	0.911
F3	2.366	0.995	0.103	0.545	1.280	0.993	10.720	0.919
F4	3.250	0.995	0.103	0.545	1.274	0.986	14.600	0.905

Results and Discussion

The yield of *Manihot esculenta* starch obtained was 43.10%, as shown in Table 2. This falls within the well-established range of 40–50%, consistent with earlier reports in the literature [28].

This further confirms the efficiency of the adapted extraction method and supports the fact that cassava is a cost-effective and abundant starch source. The slight taste and absence of odour also justify the suitability of this starch for oral delivery systems such as floating drug-delivery systems (FDDS), where patient compliance is influenced by taste, smell, and colour. The cassava starch produced a blue-black coloration with iodine solution, indicating the presence of amylose, a linear polymer responsible for swelling and gelling properties, thereby making it an appropriate polymer for FDDS [29]. The cold-water insolubility and high swelling index observed for the starch are ideal characteristics for disintegrants and may promote rapid tablet disintegration in the oral cavity [30].

Table 3 shows the flow properties of the formulated microspheres. All formulations (F1, F2, F3, and F4) displayed good flow properties, with angles of repose below 27°, consistent with Aulton and Taylor (2018), who reported that an angle of repose below 30° indicates good flowability. F1 had the highest bulk density (0.57 ± 0.01 g/cm³), suggesting better initial packing efficiency compared to the other formulations [16]. F4 exhibited the highest tapped density (0.73 ± 0.03 g/cm³), indicating good compressibility potential, while F2 showed a lower tapped density (0.67 ± 0.03 g/cm³) [16]. Regarding Hausner's ratio, F1 (1.24 ± 0.01) and F2 (1.22 ± 0.02) demonstrated good flowability, whereas F3 (1.27 ± 0.03) and F4 (1.35 ± 0.01) showed poorer flow characteristics due to their higher Hausner's ratio values (Hausner, 1967). The Carr's index values for F1, F2, and F3 were 9.72%, 17.91%, and 21.43%, respectively (Table 4), indicating acceptable flow properties. F4, with a Carr's index of 26%, exceeded the 25% threshold and thus demonstrated poor flow [8,17].

The mean particle sizes of the microspheres for the various cassava-based formulations, presented in Table 4 and Figures 1 and 2, ranged between 3.00 mm and 3.44 mm. The smaller particle sizes of F1 and F2 may enhance buoyancy and hydration rate, thereby shortening the floating lag time (Odeku et al., 2018). Morphological evaluation revealed spherical, compact microspheres. A cassava–sodium alginate blend (1:1) with sodium bicarbonate produced larger particles at a lower rotation speed (300 rpm) compared to the smaller particles obtained at a higher rotation speed (600 rpm) using a 1:2 alginate–bicarbonate ratio. This demonstrates that rotation speed significantly influences microsphere size distribution; specifically, increasing propeller speed results in smaller average particle sizes. The highest swelling index was observed in F1, at 259% (Table 4). This enhanced matrix expansion contributes to prolonged floating time, increased gastric retention, and improved drug release [3].

Received: *10-10-2025* - ***Accepted***: *08-12-2025* - ***Published***: *16-12-2025*

All four formulations floated for more than 19 hours, with F1 exhibiting the longest floating duration of 23.3 hours—exceeding the commonly cited 12-hour benchmark for FDDS. Such extended floating time supports enhanced bioavailability for drugs preferentially absorbed in the upper gastrointestinal tract due to prolonged buoyancy [3,30]. The microspheres were also evaluated for floating lag time (FLT). F1 demonstrated the shortest lag time of 2.8 minutes, indicating rapid buoyancy onset—an important attribute for immediate gastric retention. Literature consistently reports that an FLT of ≤5 minutes is optimal for FDDS performance [31]. F2 and F4 achieved significantly higher ($p \leq 0.05$) drug-entrapment efficiencies (79.2% and 81.4%, respectively), consistent with ideal FDDS characteristics for sustained release and indicative of stable polymer–drug interactions [31].

Figure 3 presents the percentage cumulative drug release over time for the control and formulations (F1–F4). All formulations showed significant, gradual, and sustained methotrexate release throughout the study period, consistent with FDDS objectives. Entrapment efficiency and cumulative drug-release ranking followed a similar pattern (F4 ≥ F2 ≥ F3 ≥ F1), in agreement with previous literature reports [32,33]. Prolonged gastric retention enhances the bioavailability of drugs absorbed in the stomach or upper intestine and reduces dosing frequency, thereby improving patient adherence.

Drug-release kinetics were analysed using zero-order, first-order, Higuchi, and Korsmeyer–Peppas models (Table 5). All formulations demonstrated excellent zero-order fit (R^2 = 0.992–0.997), while first-order fits were poor (R^2 ≈ 0.545–0.559), indicating that the release rate is not solely concentration-dependent. The Korsmeyer–Peppas model also provided a good fit (R^2 ≈ 0.986–0.993), with diffusion exponents (n = 1.254–1.300) exceeding 1.0. According to established criteria, n > 1 denotes super-case II transport, where drug release is predominantly governed by polymer relaxation and erosion rather than simple Fickian diffusion [34–38].

Conclusion

This study demonstrated that cassava (*Manihot esculenta*) starch is a suitable and efficient natural polymer for the development of floating drug-delivery systems. The four formulations investigated exhibited acceptable physicochemical characteristics, good flow properties, appropriate particle size distribution, and favourable swelling behaviour. All formulations showed rapid floating onset and prolonged buoyancy exceeding 19 hours, with F1 displaying the shortest floating lag time and longest total floating duration. Entrapment efficiency and drug-release profiles revealed that F2 and F4 achieved the highest drug loading and sustained-release behaviour, while kinetic modelling confirmed zero-order release and super-case II transport across all formulations. These findings collectively establish F1, F2, F3, and F4 as promising cassava-starch-based microsphere systems capable of enhancing gastric retention, improving methotrexate bioavailability, and supporting better patient adherence in gastroretentive drug-delivery applications.

Conflict of interest. Nil

References

1. Oyeniyi YJ, Abudulraman A. Effects of co-processing variables on properties of metronidazole tablets containing co-processed starch as sole excipient. J Pharm Bioresour. 2018;15(2):134-138. doi:10.4314/jpb.v15i2.5
2. Arora S, Kumar D, Ali J, Khar RK, Baboota S. Floating drug delivery systems: A review. AAPS PharmSciTech. 2005;6(3):E372-E390. doi:10.1208/pt060347
3. Singh BN, Kim KH. Floating drug delivery systems: an approach to oral controlled drug delivery via gastric retention. J Control Release. 2000;63(3):235-259.
4. Mishra S. Formulation and evaluation of floating tablets of methotrexate using HPMC and PEO. J Pharm Sci. 2022;106(11):3421-3428.
5. Alberta A. Methotrexate: Mechanism and pharmacokinetic challenges. Clin Pharmacol Rev. 2022;45(2):102-109.
6. Avalos-Salgado FA, Gonzalez-Lopez L, Gonzalez-Vazquez S, et al. Risk Factors Associated with Adverse Events Leading to Methotrexate Withdrawal in Elderly Rheumatoid Arthritis Patients: A Retrospective Cohort Study. *J Clin Med*. 2024;13(7):1863. doi:10.3390/jcm13071863
7. Das S, Kaur S, Rai VK. Gastro-retentive drug delivery systems: a recent update on clinical pertinence and drug delivery. Drug Deliv Transl Res. 2021;11(5):1849-1877. doi:10.1007/s13346-020-00875-5
8. Oyeniyi YJ, Gwarzo SM. Material, compressional, and mechanical properties of Borassus aethiopium (African Fanpalm) Starches. J Pharm Bioresour. 2015;12(1):8-14. doi:10.4314/jpb.v12i1.2
9. Oyewole OB, Adebayo SE, Adesina K. Physicochemical properties and functional performance of modified cassava starch. Afr J Biotechnol. 2022;21(1):22-31.
10. Odeniyi MA, Omoteso OA, Adepoju AO, Jaiyeoba KT. Starch nanoparticles in drug delivery: A review. Polim Med. 2018;48(1):41-45. doi:10.17219/pim/99993
11. Alves RMO, de Souza JAR, de Almeida CA. Cassava flour (polvilho azedo) as an alternative to wheat flour in bread making. J Food Sci. 2022;67(8):3034-3038.
12. Okunlola A, Patel RP, Odeku OA. Evaluation of freeze-dried pregelatinized Chinese yam (Dioscorea oppositifolia) starch as a polymer in floating gastroretentive metformin microbeads. J Drug Deliv Sci Technol. 2010;20(6):457-465. doi:10.1016/S1773-2247(10)50079-0

Received: *10-10-2025* - ***Accepted***: *08-12-2025* - ***Published***: *16-12-2025*

13. Salatin S, Alami-Milani M, Cilvegar H, Fereidouni S, Maghsoodi M, Monajemzadeh F, et al. Development and characterization of bilayered tablets of diazepam for oral drug delivery: design, optimization and in vitro evaluation. Ther Deliv. 2022;13(4):221-231. doi:10.4155/tde-2021-0077
14. Reddy AB, Reddy ND. Development of Multiple-Unit Floating Drug Delivery System of Clarithromycin: Formulation, in vitro Dissolution by Modified Dissolution Apparatus, in vivo Radiographic Studies in Human Volunteers. Drug Res (Stuttg). 2017;67(7):412-418. doi:10.1055/s-0043-102952
15. Reddy Dumpa N, Bandari S, Repka MA. Novel Gastroretentive Floating Pulsatile Drug Delivery System Produced via Hot-Melt Extrusion and Fused Deposition Modeling 3D Printing. Pharmaceutics. 2020;12(1):52. doi:10.3390/pharmaceutics12010052
16. United States Pharmacopeial Convention. The United States Pharmacopeia, The National Formulary (USP 43–NF 38). Rockville, MD: United States Pharmacopeial Convention; 2020. General Chapter <1174> Powder Flow.
17. Ayorinde JO, Odeniyi MA, Oyeniyi YJ. Material and Compression Properties of Native and Modified Plantain Starches. Farmacia. 2013;61(3):574-590.
18. Carr RL. Evaluating flow properties of solids. Chem Eng. 1965;72(2):163-168.
19. Marushka J, Hurychová H, Šklubalová Z, Tebbens JD. Flow Equations for Free-Flowable Particle Fractions of Sorbitol for Direct Compression: An Exploratory Multiple Regression Analysis of Particle and Orifice Size Influence. Pharmaceutics. 2022;14(8):1653. doi:10.3390/pharmaceutics14081653
20. Hausner HH. Friction conditions in a mass of metal powder. Int J Powder Metall. 1967;3(4):7-13.
21. Tan G, Morton DAV, Larson I. On the Methods to Measure Powder Flow. Curr Pharm Des. 2015;21(40):5751-5765. doi:10.2174/1381612821666151008125852
22. Aulton ME, Taylor KMG, editors. Aulton's Pharmaceutics: The Design and Manufacture of Medicines. 5th ed. Elsevier; 2018.
23. Odeku OA, Patel V, Sachan NK. Development and characterization of microspheres for pharmaceutical applications. J Microencapsul. 2023;40(1):1-11. doi:10.1080/02652048.2022.2150827
24. Oyeniyi YJ, Yusuf AJ. Quantitative effects of formulation process variables on antitumor activities of doxorubicin nanoparticles. Braz J Technol. 2019;2(4):967-983.
25. Jallo LJ, Ghoroi C, Gurumurthy L, Patel U, Davé RN. Improvement of flow and bulk density of pharmaceutical powders using surface modification. Int J Pharm. 2012;423(2):213-225. doi:10.1016/j.ijpharm.2011.12.012
26. Bade I, Karde V, Schenck L, Solomos M, Figus M, Chen C, et al. Process-Induced Crystal Surface Anisotropy and the Impact on the Powder Properties of Odanacatib. Pharmaceutics. 2024;16(7):883. doi:10.3390/pharmaceutics16070883
27. Costello MA, Liu J, Chen B, Wang Y, Qin B, Xu X, et al. Drug release mechanisms of high-drug-load, melt-extruded dexamethasone intravitreal implants. Eur J Pharm Biopharm. 2023;187:46-56. doi:10.1016/j.ejpb.2023.04.003
28. Ajani AB, Adeyemi AA, Ogunleye AO. Effect of polymer concentration on drug release profile of floating microspheres. J Pharm Sci. 2016;105(3):245-252.
29. Fu K, Zhou Y, Hou J, Shi T, Ni J, Li X, et al. Floating poly(lactic-co-glycolic acid)-based controlled-release drug delivery system for intravesical instillation. J Int Med Res. 2023;51(4):3000605231162065. doi:10.1177/03000605231162065
30. Kulkarni GT, Gowthamarajan K, Dhobe RR, Maheshwari M. Development of fast dissolving tablets of Glipizide using natural superdisintegrant. Int J Pharm Sci Rev Res. 2010;4(2):61-64.
31. Deshpande AA, Shah NH, Rhodes CT, Malick AW. Development of a novel controlled-release system for gastric retention. Pharm Res. 1997;14(6):815-819.
32. Sharma K, Thakur P, Agarwal S. Formulation and evaluation of new sustained-release floating microspheres of cilnidipine by solvent-diffusion evaporation technique. J Drug Deliv Ther. 2023;13(6):102-111. doi:10.22270/jddt.v13i6.5861
33. da Silva RYP, de Menezes DLB, Oliveira VS, Converti A, de Lima ÁAN. Microparticles in the development and improvement of pharmaceutical formulations: An analysis of in vitro and in vivo studies. Int J Mol Sci. 2023;24(6):5441. doi:10.3390/ijms24065441
34. Korsmeyer RW, Gurny R, Doelker E, Buri P, Peppas NA. Mechanisms of solute release from porous hydrophilic polymers. Int J Pharm. 1983;15(1):25-35. doi:10.1016/0378-5173(83)90064-9
35. Wu IY, Bala S, Škalko-Basnet N, di Cagno MP. Interpreting non-linear drug diffusion data: Utilizing the Korsmeyer-Peppas model to study drug release from liposomes. Eur J Pharm Sci. 2019;138:105026. doi:10.1016/j.ejps.2019.105026
36. Park C, Lee JH, Jin G, Ngo HV, Park JB, Tran TTD, et al. Release Kinetics of Hydroxypropyl Methylcellulose Governing Drug Release and Hydrodynamic Changes of Matrix Tablet. Curr Drug Deliv. 2022;19(5):520-533. doi:10.2174/1567201818666210820101549
37. Oyeniyi YJ, Nnamani ND. Preparation and Evaluation of 5 Fluorouracil Solid Dispersion Formulations for Therapeutic Management of Colorectal Cancer (CRC). Afr J Pharm Res Dev. 2018;10(2):127-134.
38. Oyeniyi YJ, Jega AM. The effects of process variables on the physicochemical properties and in-vitro cytotoxic activity of 5-Fluorouracil nanoparticles against squamous cell carcinoma (SCC). West Afr J Pharm. 2020;31(1):26-33. doi:10.60787/wapcp-31-1-196

Received*: 10-10-2025 -* ***Accepted****: 08-12-2025 -* ***Published****: 16-12-2025*